SAGE-Hindawi Access to Research
International Journal of Electrochemistry
Volume 2011, Article ID 572862, 8 pages
doi:10.4061/2011/572862

Research Article

Electrical Removal Behavior of Carbon Nanotube and Carbon Nanofiber Film in $CuCl_2$ Solution: Kinetics and Thermodynamics Study

Yankun Zhan, Chunyang Nie, Likun Pan, Haibo Li, and Zhuo Sun

Engineering Research Center for Nanophotonics and Advanced Instrument, Ministry of Education and Department of Physics, East China Normal University, Shanghai 200062, China

Correspondence should be addressed to Likun Pan, lkpan@phy.ecnu.edu.cn

Received 26 October 2010; Accepted 8 February 2011

Academic Editor: Angela Molina

The kinetics, thermodynamics, and isotherms during electrical removal of Cu^{2+} by carbon nanotube and carbon nanofiber (CNT-CNF) electrodes in $CuCl_2$ solution were studied under different solution temperatures, initial Cu^{2+} concentrations, and applied voltages. The result shows that Langmuir isotherm can describe experimental data well, indicating monolayer adsorption, and higher Cu^{2+} removal and rate constant are achieved at higher voltage, lower initial Cu^{2+} concentration, and higher solution temperature. Meanwhile, the thermodynamics analyses indicate that the electrical removal of Cu^{2+} onto CNT-CNF electrodes is mainly driven by a physisorption process.

1. Introduction

Cupric ions (Cu^{2+}) commonly exist in the waste water of several industries such as acid mine waste and acidic corrosion of pipes. The presence of excessive amounts of Cu^{2+} in drinking water may lead to accumulation in the liver and may cause gastrointestinal problems [1]. Therefore, the elimination of Cu^{2+} from water is of great importance to public health. Compared with conventional methods such as oxidation or reduction, precipitation, membrane filtration and ion exchange, electrosorption, defined as adsorption on the surface of charged electrode by applying potential or current, has been shown to be a more efficient and energy saving method to remove ions including Cu^{2+} from water since it is conducted at ambient conditions and low voltages with no secondary waste and requires no membranes, distillation columns, or thermal heaters [2–10]. Some researchers have successfully employed electrosorption to remove Cu^{2+} from solution. Oda and Nakagawa [11] investigated the removal of Cu^{2+} and Zn^{2+} using activated carbon electrodes by applying a direct voltage of 1 V. Huang and Su [12] studied the electrosorption of Cu^{2+} using activated carbon fiber cloth electrodes by imposing a low voltage of 0.3 V. Ying et al. [13] studied the electrosorption of different ions from aqueous solutions using nanostructured carbon aerogel and found a strong specific adsorption for Cu^{2+} ions. In our previous studies [14], carbon nanotube and carbon nanofiber (CNT-CNF) electrodes had been successfully used to perform the electrical removal of Cu^{2+} ions and the difficulty of their regeneration due to the electrodeposition reaction on the surface had been solved by combining reverse voltage and short circuit. When applied voltage is more than the electrodeposition potential of Cu^{2+}, the electrodeposition reaction will happen together with electrosorption of Cu^{2+} ions. The term "electrical removal" is used here considering the contribution from electrodeposition during dominant electrosorption process.

Although more and more achievements have been made on the electrical removal of dangerous Cu^{2+} ions from aqueous solution, the further detailed investigation on this field is still needed. By now, extensive papers have not paid more attention on the removal kinetics and thermodynamics which is helpful to understand the removal mechanism of Cu^{2+} ions and improve their removal efficiency from aqueous solution. In this paper, we further investigated the application of CNT-CNF films as electrodes to remove Cu^{2+}

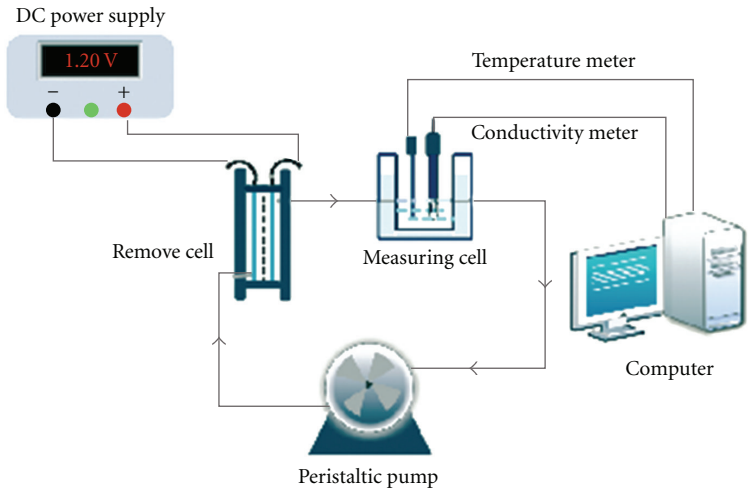

Figure 1: Schematics of batch-mode experiment.

ions from aqueous solution. Several experiments were conducted at different solution temperatures, applied potentials and initial Cu^{2+} concentrations. The corresponding removal isotherms, kinetics and thermodynamics were analyzed, respectively.

2. Experimental

2.1. Preparation and Characterization of CNT-CNF Electrodes. Graphite substrates were degreased and cleaned by acetone and alcohol, respectively. A layer of 20 nm-thick Ni catalysts was deposited on the surface of the graphite substrates by direct current (DC) magnetic sputtering (Shanghai Nanoking Co.). CNT-CNF film electrode was subsequently fabricated on the graphite substrates using the low pressure and low temperature thermal chemical vapor deposition (LPCVD) system (Shanghai Nanoking Co.). Acetylene-hydrogen ($C_2H_2 : H_2 = 1 : 5$) mixture gas was introduced into the LPCVD chamber at a flow rate of 50 and 100 sccm, respectively, at 823 K for 30 min. The surface morphology of CNT-CNF film was observed by field emission scanning electron microscopy (FESEM, JEOL S4800).

2.2. Batch-Mode Experiments. Batch-mode experiments were carried out for the Cu^{2+} removal in a continuously recycling system, as depicted in Figure 1. The system consisted of a peristaltic pump, removal cell, measuring cell, temperature meter and conductivity meter. The assembly of the removal cell was in the order: retaining plate/rubber gasket/CNT-CNF electrode/spacer/CNT-CNF electrode/rubber gasket/retaining plate. Retaining plate was made of polymethyl methacrylate. The spacing between the electrodes was maintained by rectangular nylon spacer and rubber spacer. Before the experiments, the as-grown CNT-CNF film electrodes were immersed into acid solution to dissolve the Ni particles and were packed in holders with an area of 8 cm × 8 cm and a distance of 2 mm between the electrodes. The solution was continuously pumped from the peristaltic pump into the removal cell and the effluent turned to the removal cell via measuring cell. The solution flow rate was around 40 mL/min. The analytical pure cupric chloride ($CuCl_2$) was used for the aqueous solutions. The electrical removal was performed by a DC power supply and the variation of Cu^{2+} concentrations was continuously monitored and measured in the measuring cell by using a DDS-308 ion conductivity meter (Shanghai Precision and Scientific Instrument Co. Ltd.). The relationship between conductivity and concentration was obtained according to a calibration table made prior to the experiments.

2.3. Data Analysis

2.3.1. Removal Kinetics. Generally, removal kinetics is an important characteristic of adsorbents. During the electrical removal, ion concentration gradually decreases until equilibrium is reached. This process is expected based on the large number of vacant surface sites available for electrical removal during the initial stage, and, after certain amount of time, the remaining vacant surface sites are difficult to occupy due to repulsive forces between ions on electrode and in solution. The pseudofirst-order kinetic model [15, 16] (Lagergren's equation) was employed to fit the experimental data to investigate the influence of the applied potential, solution temperature, and initial Cu^{2+} concentration on removal behavior of CNT-CNF electrodes in Cu^{2+} solution. The form of this model equation can be formulated as

$$\ln\left[\frac{C_t - C_e}{C_0 - C_e}\right] = -kt, \quad (1)$$

where k (min^{-1}) is the reaction rate constant, C_0, C_e, and C_t (mg/L) are initial concentration, equilibrium concentration, and the concentration at time t (min), respectively. The kinetics parameters can be obtained by fitting the experimental data using least square method.

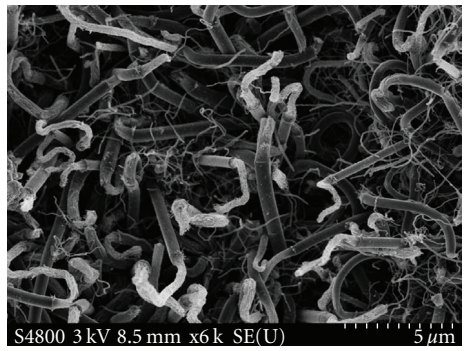

(a)

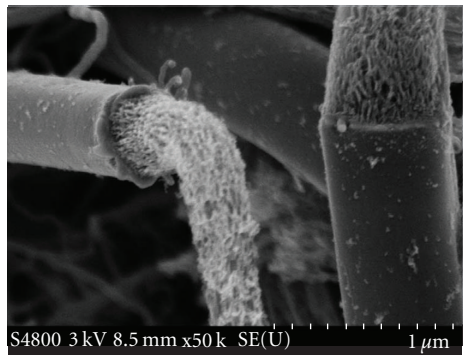

(b)

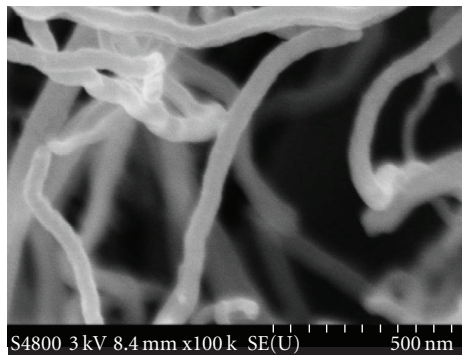

(c)

Figure 2: (a) FESEM images of CNT-CNF film, (b) CNFs, and (c) CNTs.

The change in reaction rate constant k is described by the Arrhenius equation [16, 17]:

$$\ln k = \ln A - \frac{E_a}{\mathrm{RT}}, \tag{2}$$

where A is the pre-exponential factor, R is the gas constant ($8.314\,\mathrm{Jmol^{-1}K^{-1}}$), and E_a is the activation energy. E_a and A are determined from the slope and intercept of the plot of $\ln k$ versus $1/T$.

2.3.2. Removal Isotherms. Isotherm models are used to describe the equilibrium of the adsorbate between the aqueous solution and the CNT-CNF solid phase. Langmuir isotherm model (3) and Freundlich isotherm model (4) [18] were used to fit the experimental data. Langmuir isotherm

Table 1: Cu^{2+} removal, the reaction rate constant k and correlation coefficients r^2 of kinetic equation at different applied voltages.

Voltage (V)	0	1.0	1.2	1.6	2.0
Removal (%)	10	63	72	84	90
$k\,(\mathrm{min^{-1}})$	0.0285	0.0554	0.07	0.1022	0.1055
r^2	0.9501	0.9954	0.9855	0.9926	0.9967

assumes that the single adsorbate binds to a single site on the adsorbents, and that all surface sites on the adsorbents have the same affinity for the adsorbate. The Freundlich isotherm can be derived from the Langmuir isotherm by assuming that there exists a distribution of sites on the adsorbents for different adsorbates with each site behaving accordingly to the Langmuir isotherm [19, 20]

$$q_e = \frac{q_m K_L C_\mathrm{e}}{1 + K_L C_\mathrm{e}}, \tag{3}$$

$$q_e = K_F C_e^{1/n}, \tag{4}$$

where q_e (mg/g) is the amount of adsorbed $CuCl_2$ per unit mass of CNT-CNF film and q_m (mg/g) is the maximum removal capacity corresponding to complete monolayer coverage. K_L and K_F are Langmuir constant that relates to the affinity of binding sites and Freundlich constant, respectively. q_e is calculated from the following equation:

$$q_e = \frac{(C_0 - C_e)V}{m}, \tag{5}$$

where $V(L)$ is the solution volume and m (g) is the mass of CNT-CNF film.

2.3.3. Removal Thermodynamics. The thermodynamic parameters, free energy change ΔG^0 (KJ/mol), enthalpy change ΔH^0, (KJ/mol), and entropy change ΔS^0 ($\mathrm{Jmol^{-1}K^{-1}}$), provide in-depth information on inherent energetic changes associated with electrical removal and can be determined using the following equations:

$$\begin{aligned} \Delta G^0 &= -\mathrm{RT}\ln K_L, \\ \Delta S^0 &= \frac{\Delta H^0 - \Delta G^0}{T}, \\ \ln K_L &= \frac{\Delta S^0}{R} - \frac{\Delta H^0}{\mathrm{RT}}, \end{aligned} \tag{6}$$

where $T(K)$ is absolute temperature. ΔH^0 and ΔS^0 are determined from the slope and intercept of the van't Hoff plots of $\ln K_L$ versus $1/T$ [21, 22].

2.3.4. Cu^{2+} Removal and Surface Coverage. The Cu^{2+} removal is defined as follows:

$$Cu^{2+}\ \text{Removal}\ (\%) = \frac{C_0 - C_e}{C_0} \times 100\%. \tag{7}$$

The surface coverage, defined as the ratio of the Cu^{2+} coverage per unit mass of CNT-CNF film (S_c, m^2/g) to

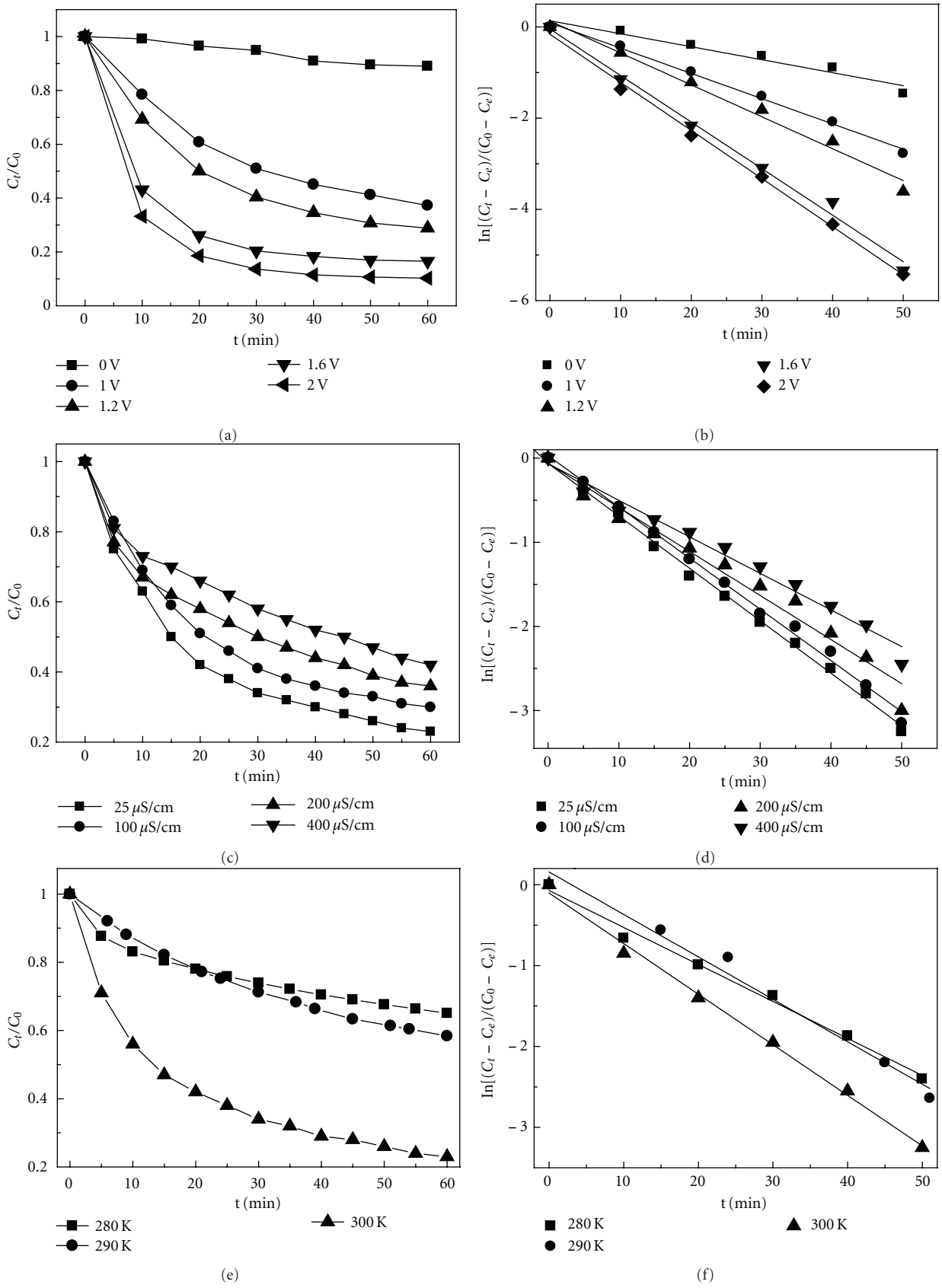

Figure 3: (a) Variation of Cu^{2+} concentration and (b) a linear plot of the first-order kinetic equation at different applied voltages; (c) variation of Cu^{2+} concentration and (d) a linear plot of the first-order kinetic equation at different initial solution conductivities; (e) variation of Cu^{2+} concentration and (f) a linear plot of the first-order kinetic equation during batch mode experiments at different solution temperatures.

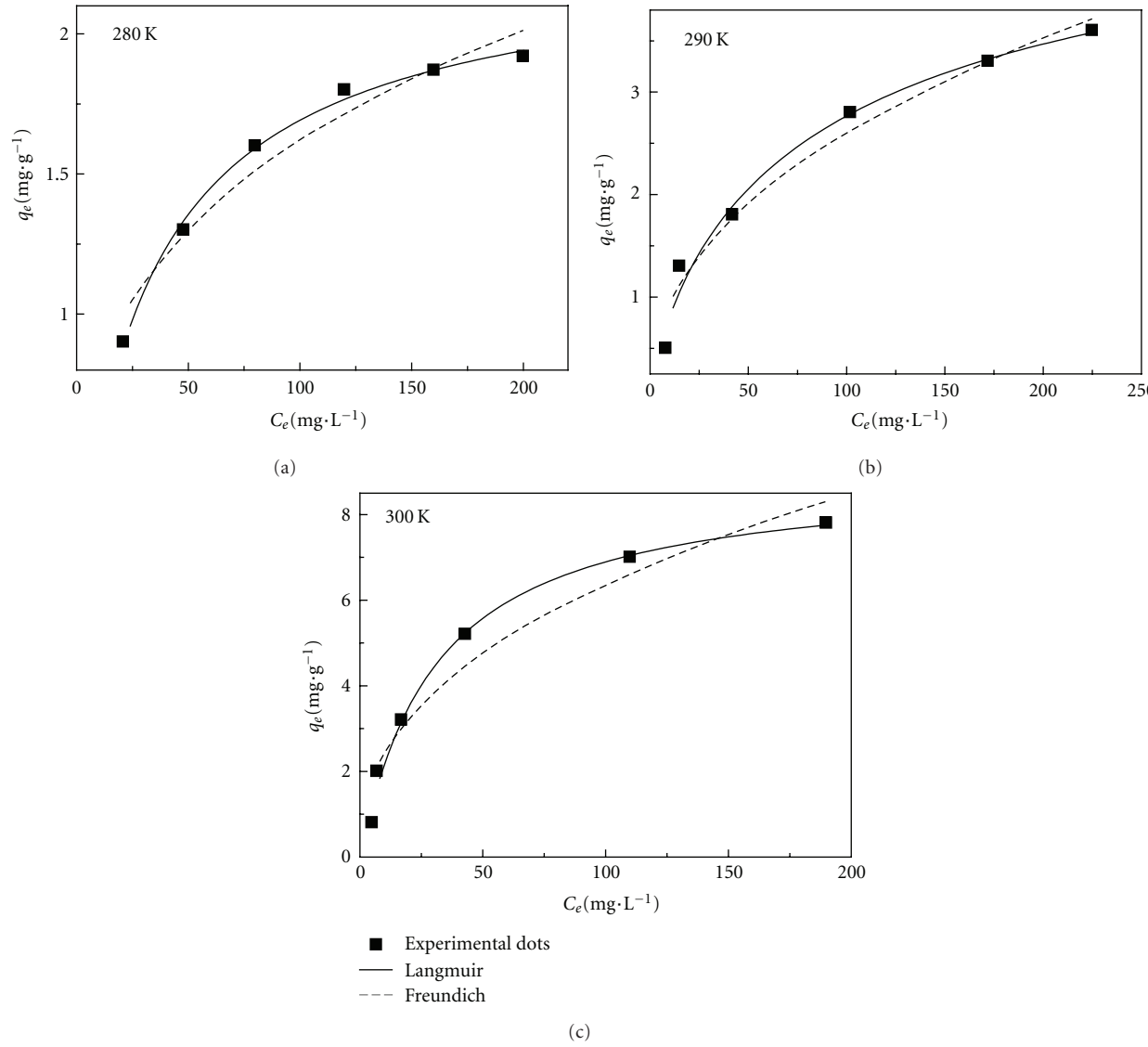

Figure 4: Equilibrium isotherms of CNT-CNF film electrodes in $CuCl_2$ solution at (a) 280 K, (b) 290 K and (c) 300 K.

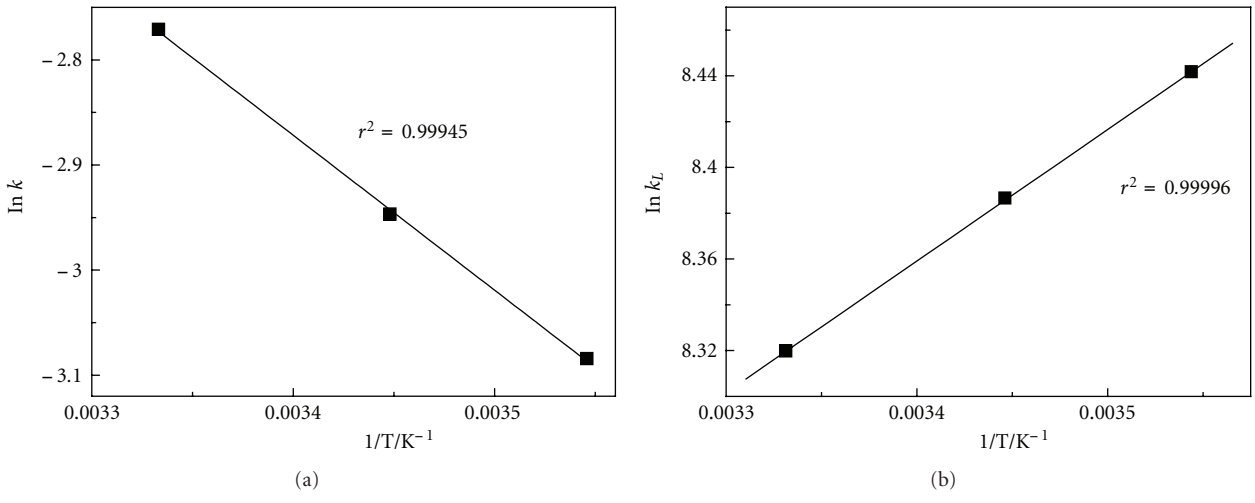

Figure 5: (a) Linear plot of ln k versus 1/T and (b) van't Hoff plot for the electrical removal of $CuCl_2$ onto CNT-CNF film electrodes.

Table 2: Cu^{2+} removal, the reaction rate constant k and correlation coefficients r^2 of kinetic equation at different initial solution conductivities and different solution temperatures.

	Initial solution conductivity (μS/cm)				Temperature (K)		
	25	100	200	400	280	290	300
Removal (%)	77	70	64	58	35	42	70
k (min^{-1})	0.0624	0.0609	0.0524	0.0435	0.0457	0.0525	0.0626
r^2	0.9967	0.9952	0.9694	0.9773	0.9918	0.9830	0.9954

Table 3: Parameters determined from Langmuir and Freundlich isotherms of CNT-CNF film electrodes in $CuCl_2$ solution (q_e is the amount of adsorbed $CuCl_2$ per unit mass of CNT-CNF film; q_m is the maximum removal capacity corresponding to complete monolayer coverage; K_L and K_F are Langmuir constant and Freundlich constant; r^2 is correlation coefficients).

Isotherm	Model equation	Parameter	280 K	290 K	300 K
Langmuir	$q_e = (q_m K_L C_e)/(1 + K_L C_e)$	q_m (mg/g)	2.30	5.38	8.96
		K_L (L/mg)	0.0345	0.0326	0.0305
		r^2	0.9963	0.9852	0.9918
Freundlich	$q_e = K_F C_e^{1/n}$	K_F	0.3848	0.34	0.9309
		$1/n$	0.3122	0.4415	0.4172
		r^2	0.9584	0.9728	0.9483

Table 4: The free energy change ΔG^0, enthalpy change ΔH^0 and entropy change ΔS^0 for electrical removal of CNT-CNF film electrodes in $CuCl_2$ solutions.

T (K)	ΔG^0 (KJ/mol)	ΔH^0 (KJ/mol)	ΔS^0 (J/molK)
280	−19.80		
290	−20.30	−4.774	53.27
300	−20.76		

the BET surface area of CNT-CNF film (S_p, m^2/g), is helpful in understanding the interaction between adsorbates and the surfaces of adsorbents and can be calculated as follows [23]:

$$\frac{S_c}{S_p(\%)} = \frac{N_A A_m q_m}{1000 S_p M_w} \times 100\%, \quad (8)$$

where A_m (m^2) is the maximum cross-section area of adsorbate molecule or ion. M_w is the molecular weight of adsorbate.

3. Results and Discussion

Figures 2(a)–2(c) show the FESEM images of CNT-CNF film, CNFs, and CNTs, respectively. It can be found that CNF with a diameter of around 600 nm consists of core palpus and a carbon layer sheath outside and serves as the frame for the CNT growth. The CNTs and CNFs are entangled and form a continuous electroconducting network microstructure. There are many mesoporous pores between CNTs and CNFs and their sizes are distributed from 4 nm to 30 nm [24]. Such a network structure ensures a low mass-transfer and allows hydrated ions easily to enter through the pores of the CNT-CNF film which were very helpful for the ion adsorption [25, 26].

Figures 3(a) and 3(b) show the variation of Cu^{2+} concentration and a linear plot of the first-order kinetic equation between the concentration terms *versus* time during batch mode experiments at five different applied voltages of 0, 1.0, 1.2, 1.6, and 2.0 V, respectively. All the charge processes are carried out for 60 minutes. The solution temperature is 290 K and the initial solution conductivity is 50 μS/cm. Table 1 summarizes the Cu^{2+} removal and the estimated coefficients of kinetic equation at different applied voltages. Under the potential ranges between 0 and 2.0 V, Cu^{2+} removal and rate constant increase from 0.0285 min^{-1} and 10% to 0.1055 min^{-1} and 90%, respectively. Nevertheless, hydrolysis of water is not found when the voltage between the two electrodes is less than 2.0 V because of the existence of resistance in the whole circuit. Obviously, the electrical removal is dependent on applied voltage and higher Cu^{2+} removal and rate constant are achieved at higher voltage due to stronger electrostatic force to drive Cu^{2+} onto CNT-CNF film.

Figures 3(c) and 3(d) display the variation of Cu^{2+} concentration and a linear plot of the first-order kinetic equation between the concentration terms *versus* time during batch mode experiments with different initial solution conductivities of 25, 100, 200, and 400 μS/cm, respectively. All the charge processes are carried out for 60 minutes. The solution temperature is 300 K and the applied voltage is 1.2 V. Table 2 summarizes the Cu^{2+} removal and the estimated coefficients of kinetic equation with different initial solution conductivities. It can be observed that the Cu^{2+} removal and rate constant decrease with the increase in initial solution conductivity, that is, initial Cu^{2+} concentration. The lower rate constant in solution with higher initial Cu^{2+} concentration may be due to higher coulomb repulsion, while the lower Cu^{2+} removal is ascribed to the lack of available active sites on the CNT-CNF surface which is quickly saturated with ion species [27].

Figures 3(e) and 3(f) show the variation of Cu^{2+} concentration and a linear plot of the first-order kinetic equation

between the concentration terms *versus* time during batch mode experiments at different solution temperatures of 280, 290, and 300 K, respectively. All the charge processes are carried out for 60 minutes. The applied voltage is 1.2 V and the initial solution conductivity is 100 μS/cm. As shown in Table 2, the Cu^{2+} removal and rate constant increase with the increase in solution temperature. This should be due to the availability of more active sites on the surface of CNT-CNF at higher temperature [28].

Electrical removal experiments with different initial solution conductivities (25–400 μs/cm) at 280, 290, and 300 K were carried out to obtain the isotherm. The applied voltage is 1.2 V. Figures 4(a)–4(c) show the removal isotherms at 280, 290 and 300 K, respectively. The determined parameters and regression coefficients r^2, K_L, and K_F of Langmuir and Freundlich isotherms are given in Table 3. The r^2 of Langmuir model at each temperature is larger than that of Freundlich model, which indicates Langmuir isotherm better describes the experimental data and suggests that for modeling purposes, monolayer coverage of the CNT-CNF film surface area and equal activation energy during electrical removal process can be assumed [29].

The activation energy E_a was calculated to be 12.256 KJ/mol from the slope of linear plot of ln$k$ versus $1/T$, as shown in Figure 5(a). Such a value (5–40 KJ/mol) is characteristic for a diffusion and physisorption controlled process [30], suggesting that the Cu^{2+} ions are removed mainly due to the electrical double layer effect although the existence of electrodeposition reaction. Figure 5(b) shows the van't Hoff plot for the electrical removal of $CuCl_2$ onto CNT-CNF electrodes. Table 4 presents the thermodynamic parameters at 280, 290, and 300 K. The ΔG^0 values are negative at all testing temperatures, verifying that the electrical removal of $CuCl_2$ onto CNT-CNF is thermodynamically favorable. In other words, a more negative ΔG^0 implies a greater driving force, resulting in an increased electrical removal performance. As temperature increases from 280 K to 300 K, ΔG^0 decreases negatively, suggesting that the electrical removal is more favorable at high temperatures. The negative ΔH^0 indicates that electrical removal of $CuCl_2$ onto CNT-CNF is an exothermic process [28, 31, 32] and the positive ΔS^0 represents that the degrees of freedom increase at the solid-liquid interface during electrical removal [33]. Physisorption and chemisorption can be classified, to a certain extent, by the magnitude of enthalpy change ΔH^0. $\Delta H^0$of <40 kJ/mol are typically considered as those of physisorption bonds [34, 35]. Generally, ΔG^0 for physisorption is less than that for chemisorption. The former is between −20 and 0 kJ/mol and the latter is between −80 and −400 kJ/mol [36]. Therefore, both of ΔH^0 and ΔG^0 suggest that electrical removal of $CuCl_2$ onto CNT-CNF is mainly driven by a physisorption process although the existence of electrodeposition reaction.

The BET specific surface area S_p of CNT-CNF is 210 m^2/g. A_m is calculated based on the hydrated Cu^{2+} ion radius (6×10^{-10} m). Therefore, the monolayer coverage area of the CNT-CNF surface by Cu^{2+} at 280, 290, and 300 K, calculated from (8) are 5.6%, 13%, and 21.7%, respectively. The surface coverage of CNT-CNF by hydrated Cu^{2+} ions increases with the increase of temperature, indicating that more Cu^{2+} ions are removed at high temperature.

4. Conclusion

The CNT-CNF electrodes were fabricated using LPCVD method and their electrical removal behaviors including kinetics, thermodynamics, and isotherms in $CuCl_2$ solution were studied. The result shows that (i) the electrical removal follows Langmuir isotherm, indicating monolayer adsorption; (ii) higher voltage, lower initial Cu^{2+} concentration and higher solution temperature can enhance Cu^{2+} removal and facilitate rate constant; (iii) electrical removal of $CuCl_2$ onto CNT-CNF can be mainly ascribed to physisorption process.

Acknowledgments

This paper was supported by Special Project for Nanotechnology of Shanghai (no. 1052nm02700) and the Scientific Research Foundation for the Returned Overseas Chinese Scholars.

References

[1] M. Goyal, V. K. Rattan, D. Aggarwal, and R. C. Bansal, "Kinetics of adsorption and desorption of Pb(II) in aqueous solution on activated carbon by two-site adsorption model," *Colloids and Surfaces A*, vol. 190, pp. 229–238, 2001.

[2] T. J. Welgemoed and C. F. Schutte, "Capacitive deionization technology (TM): an alternative desalination solution," *Desalination*, vol. 183, no. 1–3, pp. 327–340, 2005.

[3] K. Y. Foo and B. H. Hameed, "Value-added utilization of oil palm ash: a superior recycling of the industrial agricultural waste," *Journal of Hazardous Materials*, vol. 170, no. 2-3, pp. 552–559, 2009.

[4] H. Li, T. Lu, L. Pan, Y. Zhang, and Z. Sun, "Electrosorption behavior of graphene in NaCl solutions," *Journal of Materials Chemistry*, vol. 19, no. 37, pp. 6773–6779, 2009.

[5] M. A. Anderson, A. L. Cudero, and J. Palma, "Capacitive deionization as an electrochemical means of saving energy and delivering clean water. Comparison to present desalination practices: will it compete?" *Electrochimica Acta*, vol. 55, no. 12, pp. 3845–3856, 2010.

[6] M. Andelman, "The flow through capacitor: a new tool in wastewater purification," *Filtration and Separation*, vol. 35, pp. 345–348, 1998.

[7] Y. Oren, "Capacitive deionization (CDI) for desalination and water treatment—past, present and future (a review)," *Desalination*, vol. 228, no. 1–3, pp. 10–29, 2008.

[8] S. J. Seo, H. Jeon, J. K. Lee et al., "Investigation on removal of hardness ions by capacitive deionization (CDI) for water softening applications," *Water Research*, vol. 44, no. 7, pp. 2267–2275, 2010.

[9] H. J. Oh, J. H. Lee, H. J. Ahn, Y. Jeong, Y. J. Kim, and C. S. Chi, "Nanoporous activated carbon cloth for capacitive deionization of aqueous solution," *Thin Solid Films*, vol. 515, no. 1, pp. 220–225, 2006.

[10] D. Zhang, L. Shi, J. Fang, K. Dai, and X. Li, "Preparation and desalination performance of multiwall carbon nanotubes," *Materials Chemistry and Physics*, vol. 97, no. 2-3, pp. 415–419, 2006.

[11] H. Oda and Y. Nakagawa, "Removal of ionic substances from dilute solution using activated carbon electrodes," *Carbon*, vol. 41, no. 5, pp. 1037–1047, 2003.

[12] C. C. Huang and Y. J. Su, "Removal of copper ions from wastewater by adsorption/electrosorption on modified activated carbon cloths," *Journal of Hazardous Materials*, vol. 175, no. 1–3, pp. 477–483, 2010.

[13] T. Y. Ying, K. L. Yang, S. Yiacoumi, and C. Tsouris, "Electrosorption of ions from aqueous solutions by nanostructured carbon aerogel," *Journal of Colloid and Interface Science*, vol. 250, no. 1, pp. 18–27, 2002.

[14] Y. Zhan, H. Li, L. Pan, Y. Zhang, Y. Chen, and Z. Sun, "Regeneration of carbon nanotube and nanofibre composite film electrode for electrical removal of cupric ions," *Water Science and Technology*, vol. 61, no. 6, pp. 1427–1432, 2010.

[15] S. Langergren and B. K. Svenska, "Zur theorie der sogenannten adsorption geloester stoffe," *Handlingar*, vol. 24, pp. 1–39, 1898.

[16] A. Y. Dursun and C. S. Kalayci, "Equilibrium, kinetic and thermodynamic studies on the adsorption of phenol onto chitin," *Journal of Hazardous Materials*, vol. 123, no. 1–3, pp. 151–157, 2005.

[17] C. H. Wu, "Studies of the equilibrium and thermodynamics of the adsorption of Cu^{2+} onto as-produced and modified carbon nanotubes," *Journal of Colloid and Interface Science*, vol. 311, no. 2, pp. 338–346, 2007.

[18] S. Wang, D. Wang, L. Ji, Q. Gong, Y. Zhu, and J. Liang, "Equilibrium and kinetic studies on the removal of NaCl from aqueous solutions by electrosorption on carbon nanotube electrodes," *Separation and Purification Technology*, vol. 58, no. 1, pp. 12–16, 2007.

[19] I. Langmuir, "The adsorption of gases on plane surfaces of glass, mica and platinum," *The Journal of the American Chemical Society*, vol. 40, no. 9, pp. 1361–1403, 1918.

[20] T. S. Anirudhan and P. G. Radhakrishnan, "Chromium(III) removal from water and wastewater using a carboxylate-functionalized cation exchanger prepared from a lignocellulosic residue," *Journal of Colloid and Interface Science*, vol. 316, no. 2, pp. 268–276, 2007.

[21] Y. J. Zhang, J. R. Chen, X. Y. Yan, and Q. M. Feng, "Equilibrium and kinetics studies on adsorption of Cu(II) from aqueous solutions onto a graft copolymer of cross-linked starch/acrylonitrile (CLSAGCP)," *Journal of Chemical Thermodynamics*, vol. 39, no. 6, pp. 862–865, 2007.

[22] A. S. Ozcan, B. Erdem, and A. Ozcan, "Adsorption of Acid Blue 193 from aqueous solutions onto Na-bentonite and DTMA-bentonite," *Journal of Colloid and Interface Science*, vol. 280, no. 1, pp. 44–54, 2004.

[23] R. L. Tseng and S. K. Tseng, "Characterization and use of high surface area activated carbons prepared from cane pith for liquid-phase adsorption," *Journal of Hazardous Materials*, vol. 136, no. 3, pp. 671–680, 2006.

[24] X. Z. Wang, M. G. Li, Y. W. Chen et al., "Electrosorption of ions from aqueous solutions with carbon nanotubes and nanofibers composite film electrodes," *Applied Physics Letters*, vol. 89, no. 5, Article ID 053127, 2006.

[25] Y. Gao, L. Pan, H. Li et al., "Electrosorption behavior of cations with carbon nanotubes and carbon nanofibres composite film electrodes," *Thin Solid Films*, vol. 517, no. 5, pp. 1616–1619, 2009.

[26] D. Zhang, L. Shi, J. Fang, K. Dai, and J. Liu, "Influence of carbonization of hot-pressed carbon nanotube electrodes on removal of NaCl from saltwater solution," *Materials Chemistry and Physics*, vol. 96, no. 1, pp. 140–144, 2006.

[27] G. N. Manju, C. Raji, and T. S. Anirudhan, "Evaluation of coconut husk carbon for the removal of arsenic from water," *Water Research*, vol. 32, no. 10, pp. 3062–3070, 1998.

[28] A. Ozcan, A. S. Ozcan, S. Tunali, T. Akar, and I. Kiran, "Determination of the equilibrium, kinetic and thermodynamic parameters of adsorption of copper(II) ions onto seeds of Capsicum annuum," *Journal of Hazardous Materials*, vol. 124, no. 1–3, pp. 200–208, 2005.

[29] A. K. Yadav, C. P. Kaushik, A. K. Haritash, A. Kansal, and N. Rani, "Defluoridation of groundwater using brick powder as an adsorbent," *Journal of Hazardous Materials*, vol. 128, no. 2-3, pp. 289–293, 2006.

[30] K. Banerjee, P. N. Cheremisinoff, and SU. L. Cheng, "Adsorption kinetics of o-xylene by flyash," *Water Research*, vol. 31, no. 2, pp. 249–261, 1997.

[31] J. W. Kim, M. H. Sohn, D. S. Kim, S. M. Sohn, and Y. S. Kwon, "Production of granular activated carbon from waste walnut shell and its adsorption characteristics for Cu^{2+} ion," *Journal of Hazardous Materials*, vol. 85, no. 3, pp. 301–315, 2001.

[32] Y. Prasanna Kumar, P. King, and V. S. R. K. Prasad, "Equilibrium and kinetic studies for the biosorption system of copper(II) ion from aqueous solution using Tectona grandis L.f. leaves powder," *Journal of Hazardous Materials*, vol. 137, no. 2, pp. 1211–1217, 2006.

[33] G. Uslu and M. Tanyol, "Equilibrium and thermodynamic parameters of single and binary mixture biosorption of lead (II) and copper (II) ions onto Pseudomonas putida: effect of temperature," *Journal of Hazardous Materials*, vol. 135, no. 1–3, pp. 87–93, 2006.

[34] M. Alkan, O. Demirbas, S. Celikcapa, and M. Doğan, "Sorption of acid red 57 from aqueous solution onto sepiolite," *Journal of Hazardous Materials*, vol. 116, no. 1-2, pp. 135–145, 2004.

[35] S. D. Faust and O. M. Aly, *Adsorption Processes for Water Treatment*, Butterworth, 1987.

[36] M. J. Jaycock and G. D. Parfitt, *Chemistry of Interfaces*, Ellis Horwood, Chichester, UK, 1981.